

The reaction of alkynes with *triangulo*-clusters [Pt₃(μ-CO)₃(PR₃)₃]Renzo Ros,^{*a} Augusto Tassan,^a Raymond Roulet,^{*b} Virginie Duprez,^b Serena Detti,^b Gábor Laurenczy^b and Kurt Schenk^c^a Dipartimento di Processi Chimici dell'Ingegneria, Via Marzolo 9, I-35131 Padova, Italy^b Institut de Chimie Minérale et Analytique de l'Université, BCH, CH-1015 Lausanne, Switzerland^c Institut de Cristallographie de l'Université, BSP, CH-1015 Lausanne, Switzerland

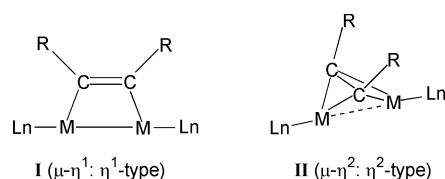
Received 12th April 2001, Accepted 25th July 2001

First published as an Advance Article on the web 31st August 2001

The reaction of the cluster complexes [Pt₃(μ-CO)₃(PR₃)₃] (PR₃ = PPh₃ **1**, PPh₂Bz **2**, PCy₃ **3** and PⁱPr₃ **4**) with dialkyl acetylenedicarboxylate, R'O₂CC≡CCO₂R' (R' = CH₃ or ^tBu) have been examined under various conditions. At low temperature the alkyne reacts quantitatively giving the unstable adducts [Pt₃(CO)₃(PR₃)₃(μ₃-alkyne)]. The stereochemistry of the intermediate [Pt₃(CO)₃(PPh₃)₃(μ₃-^tBuO₂CC≡CCO₂^tBu)] **5** has been deduced from low temperature ¹⁹⁵Pt-¹H, ³¹P-¹H and ¹³C-¹H NMR spectra. At higher temperature a fluxional process renders two of the three platinum atoms equivalent on the NMR timescale. At room temperature the alkynes convert the starting clusters **1–4** to the stable dinuclear complexes [Pt₂(CO)₂(PR₃)₂(μ-R'O₂CC≡CCO₂R')] (R' = CH₃, PR₃ = PPh₃ **6**; R = ^tBu, PR₃ = PPh₃ **7**; PPh₂Bz **8**; PCy₃ **9** and PⁱPr₃ **10**) in which the alkyne coordination has the C–C bond collinear with the Pt–Pt bond (**6** and **7**) or perpendicular to the Pt–Pt axis (**9** and **10**). The stereochemistry of these two types of dinuclear complexes has been established by NMR and IR studies and confirmed by X-ray diffraction analyses of **8** and **9**.

Introduction

The interaction of olefins and alkynes with metal surfaces is important for heterogeneous catalysis.^{1,2} Since there is a remarkable resemblance between the ways in which small molecules bind to the coordinatively unsaturated platinum cluster complexes and a Pt-surface,^{3,4} a study of the coordination of organic species to [Pt₃(μ-CO)₃(PR₃)₃] (PR₃ = PPh₃ **1**, PPh₂Bz **2**, PCy₃ **3** and PⁱPr₃ **4**)^{5–9} should be a useful model for substrate chemisorption in heterogeneous catalysis. For mononuclear complexes the binding of simple substrates, such as olefins and alkynes, is well understood and can be readily rationalised based on the Dewar–Chatt–Duncanson model.¹⁰ However, for complexes which involve more than one metal center, additional complexity is introduced owing to the presence of adjacent metals and hence the possibility of bridging modes for the substrate molecule. For dinuclear complexes two geometries have been found to occur, one with the carbon–carbon bond collinear to the M–M bond, the other perpendicular (structures **I** and **II**, respectively).¹¹ Interconversion of these two bonding modes has also been proposed for the [Pt₂(μ-CF₃C≡CCF₃)(COD)]₂ complex.¹²



Recently, we have described the reactions of *triangulo*-cluster compounds of platinum [Pt₃(μ-CO)₃(PR₃)₃] with sulfur dioxide¹³ and activated olefins,¹⁴ giving [Pt₃(μ-SO₂)_n(μ-CO)_{3-n}(PR₃)₃] (*n* = 1–3) and [Pt(CO)(PR₃)(olefin)], respectively, the latter *via* the adduct [Pt₃(μ-CO)₃(PR₃)₃(olefin)].

In this paper we describe the reactivity of some trinuclear clusters with acetylenes. The unstable intermediate adducts,

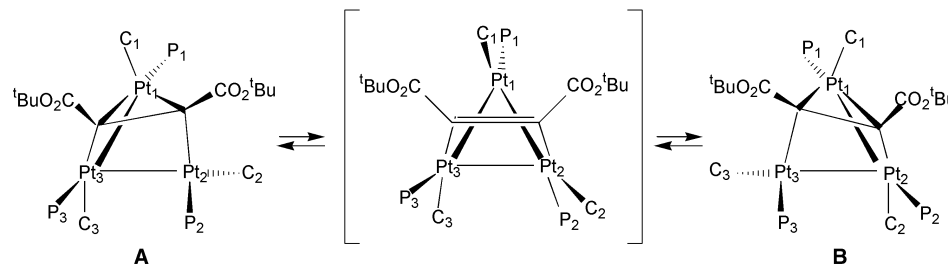
identified at low temperature, slowly rearrange to dinuclear acetylene-bridged complexes of μ-η¹:η¹- or μ-η²:η²- types.

Results and discussion

Spectroscopic evidence for the adduct [Pt₃(CO)₃(PPh₃)₃(μ₃-^tBuO₂CC≡CCO₂^tBu)] **5**

The addition reaction between an equimolar amount of di(*tert*-butyl)acetylenedicarboxylate and [Pt₃(μ-CO)₃(PPh₃)₃] **1** occurs rapidly in CH₂Cl₂ below –50 °C to give a red-brown solution of the adduct [Pt₃(μ-CO)₃(PPh₃)₃(μ₃-η¹:η¹:η²-^tBuO₂CC≡CCO₂^tBu)] **5**. Attempts to isolate this adduct were unsuccessful, due to disproportionation to the starting *triangulo*-cluster **1** and the dimeric complex [Pt₂(CO)₂(PPh₃)₂(μ-η¹:η¹-^tBuO₂CC≡CCO₂^tBu)] **7**. The ³¹P-¹H NMR spectrum at –80 °C shows three resonances of approximately equal intensity with satellites, indicative of three non-equivalent phosphine environments in a trinuclear complex having only two Pt–Pt bonds (Fig. 1 and Table 1). The spectrum is a superposition of the subspectra related to eight isotopomers, *i.e.* one without ¹⁹⁵Pt (29.01% abundance), three isotopomers containing one ¹⁹⁵Pt nucleus (14.81% each), three isotopomers with two ¹⁹⁵Pt (7.56% each) and one with three ¹⁹⁵Pt nuclei (3.86%). A computer simulation using the program gNMR 4.0 has confirmed the assignment of the coupling constants.¹⁵ Warming the solution causes reversible changes in the satellite pattern of the P₁ resonance, with a simultaneous broadening of the signals at 17.5 and 27.2 ppm (P₂ and P₃, respectively) and a shift of both resonances ending in coalescence at 21.5 ppm (Fig. 1).

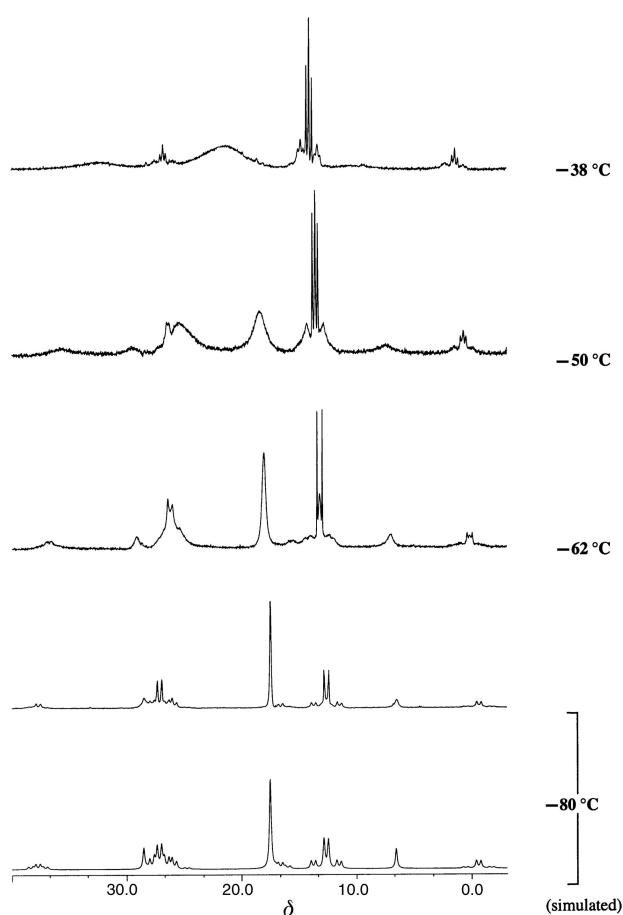
The ¹³C-¹H NMR spectrum of a ¹³CO enriched (>99%) sample of **5**, in CD₂Cl₂ at –86 °C also contains signals for three non-equivalent carbonyl ligands with satellites, located in the region of terminal COs. Formally this unsymmetrical adduct, having a μ₃-η¹:η¹:η²-alkyne bonding mode, is a 46-electron cluster and should thus contain only two Pt–Pt bonds (Scheme in Table 1). Its ¹³C-¹H variable temperature NMR shows a broadening of the signal at 178.2 (C₂) and 189.9 ppm (C₃) upon

Table 1 Variable temperature ^{31}P - $\{^1\text{H}\}$ and ^{13}C NMR data for $[\text{Pt}_3(\text{CO})_3(\text{PPh}_3)_3(\mu_3\text{-}^t\text{BuO}_2\text{CC}\equiv\text{CCO}_2^t\text{Bu})]$ **5** in CD_2Cl_2 (δ/ppm ; J/Hz)


$T/^\circ\text{C}$	$\delta(\text{P}_1)$	$\delta(\text{P}_2)$	$\delta(\text{P}_3)$	$^1J(\text{P}_1\text{-Pt}_1)$	$^1J(\text{P}_2\text{-Pt}_2)$	$^1J(\text{P}_3\text{-Pt}_3)$	$^2J(\text{P}_1\text{-Pt}_3)$	$^2J(\text{P}_3\text{-Pt}_1)$	$^3J(\text{P}_1\text{-P}_3)$	$^3J(\text{P}_2\text{-P}_3)$	$^4J(\text{P}_1\text{-P}_2)$
-80	12.66	17.53	27.16	4283	3565	3406	362	207	62	6	8
-74	13.22	17.72	26.96	4268	3568	3408	361	207	61	<i>a</i>	<i>a</i>
-50	13.64	18.45	25.40	4177	≈ 3560	≈ 3330	234	207	42	<i>a</i>	<i>a</i>
-38	14.14	21.49		4107	<i>a</i>	<i>a</i>	238	<i>a</i>	40	<i>a</i>	<i>a</i>

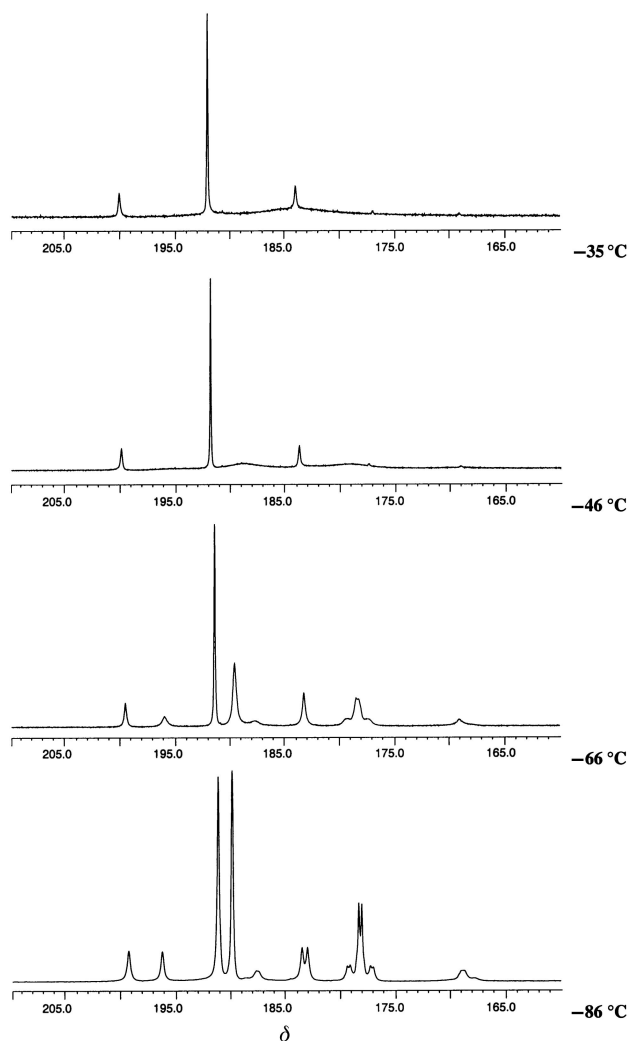
	$\delta(\text{C}_1)$	$\delta(\text{C}_2)$	$\delta(\text{C}_3)$	$^1J(\text{C}_1\text{-Pt}_1)$	$^1J(\text{C}_2\text{-Pt}_2)$	$^1J(\text{C}_3\text{-Pt}_3)$	$^2J(\text{C}_2\text{-Pt}_3)$	$^3J(\text{C}_2\text{-P}_3)$
-86	191.2	178.2	189.9	1634	1886	1281	211	28.1
-66	191.5	178.4	189.6	1633	1873	1279	199	23
-46	191.9	179.4	189.0	1624	<i>a</i>	<i>a</i>	<i>a</i>	<i>a</i>
-35	192.1	184.2		1612	<i>a</i>	<i>a</i>	<i>a</i>	<i>a</i>

a Not observed.

**Fig. 1** Variable temperature and simulated (-80°C) ^{31}P - $\{^1\text{H}\}$ NMR spectra (161.93 MHz) of adduct $[\text{Pt}_3(\text{CO})_3(\text{PPh}_3)_3(\mu_3\text{-}^t\text{BuO}_2\text{CC}\equiv\text{CCO}_2^t\text{Bu})]$, **5**, in CD_2Cl_2 .

heating which is accompanied by a convergent shift of resonances to 184.2 ppm; the coalescence temperature was estimated at *ca.* -30°C (Fig. 2).

The non-rigid structure of adduct **5** is confirmed by the ^{195}Pt - $\{^1\text{H}\}$ NMR spectrum in CD_2Cl_2 at -95°C , which shows only the resonance of Pt_1 (-4427 ppm) as a doublet of doublets, due

**Fig. 2** Variable temperature ^{13}C - $\{^1\text{H}\}$ NMR spectra (99.55 MHz) of adduct $[\text{Pt}_3(^{13}\text{CO})_3(\text{PPh}_3)_3(\mu_3\text{-}^t\text{BuO}_2\text{CC}\equiv\text{CCO}_2^t\text{Bu})]$, **5**, in CD_2Cl_2 .

to the $\text{P}_1\text{-}^{195}\text{Pt}_1\text{-Pt}_2\text{-P}_2$ and $\text{P}_1\text{-}^{195}\text{Pt}_1\text{-Pt}_3\text{-P}_3$ equivalent isotopomers ($^1J(\text{Pt}_1\text{-P}) = 3414$ Hz, $^2J(\text{Pt}_1\text{-P}) = 372$ Hz), flanked by low intensity signals arising from the subspectrum for the

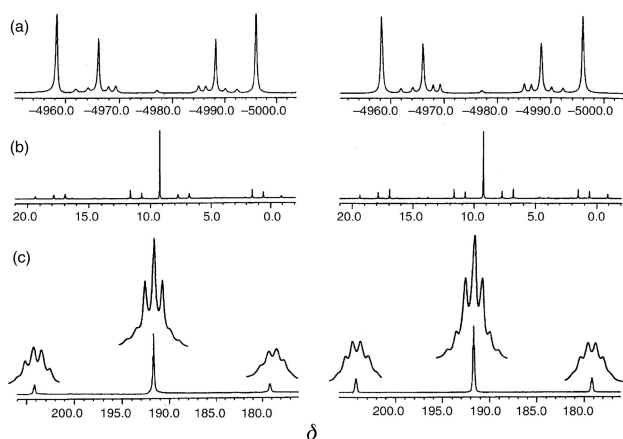


Fig. 3 Observed (left) and simulated (right) spectra of $[\text{Pt}_2(\text{CO})_2(\text{PPh}_2\text{Bz})_2(\mu\text{-}\eta^1\text{-}\eta^1\text{-}^t\text{BuO}_2\text{CC}\equiv\text{CCO}_2^t\text{Bu})]$, **8**, in CD_2Cl_2 at 25°C : (a) $^{195}\text{Pt}\text{-}\{^1\text{H}\}$ (77.38 MHz), (b) $^{31}\text{P}\text{-}\{^1\text{H}\}$ (161.93 MHz) and (c) $^{13}\text{C}\text{-}\{^1\text{H}\}$ NMR (50.32 MHz), the latter for the ^{13}C enriched (>99%) complex.

$\text{P}_1\text{-}^{195}\text{Pt}_1\text{-}^{195}\text{Pt}_2\text{-}\text{P}_2$ and the symmetrically equivalent $\text{P}_1\text{-}^{195}\text{Pt}_1\text{-}^{195}\text{Pt}_3\text{-}\text{P}_3$ isotopomer (see **A** and **B** in Table 1), which allow an estimation of the $^{195}\text{Pt}\text{-}^{195}\text{Pt}$ coupling constant as *ca.* 1021 Hz. No signals for the other two Pt atoms were detected. At higher temperature this single signal broadens, and disappears into the base line above -70°C . This type of dynamic process involving trinuclear platinum acetylene complexes has not been previously observed. The site exchange mechanism of $[\text{Pt}(\text{CO})_3(\text{PCy}_3)_3(\text{MeO}_2\text{CC}\equiv\text{CCO}_2\text{Me})]$ has not been ascertained, and another type of dynamic process, *i.e.* the rotation of the acetylenic ligand above one of the Pt_3 faces of $[\text{Pt}_6(\text{CO})_6(\mu\text{-dpmp})_2(\text{MeO}_2\text{CC}\equiv\text{CCO}_2\text{Me})]$ has been reported recently.^{16b} The **A** \rightleftharpoons **B** exchange proposed in Table 1 explains the dynamics which renders the Pt_2 and Pt_3 environments equivalent on the NMR timescale. Unfortunately no other acetylene adduct of the other *triangulo*-cluster complexes could be observed in the slow exchange domain.

Synthesis and characterisation of dinuclear complexes $[\text{Pt}_2(\text{CO})_2(\text{PR}_3)_2(\mu\text{-alkyne})]$

Excess of dialkyl acetylenedicarboxylate, $\text{R}'\text{O}_2\text{CC}\equiv\text{CCO}_2\text{R}'$ ($\text{R}' = \text{CH}_3$ or ^tBu) reacts at room temperature with $[\text{Pt}_3(\mu\text{-CO})_3(\text{PR}_3)_3]$ ($\text{PR}_3 = \text{PPh}_3, \text{PPh}_2\text{Bz}, \text{PCy}_3$ and P^iPr_3) to give not the expected monoplatinum(0) complexes $[\text{Pt}(\text{CO})(\text{PR}_3)(\text{R}'\text{O}_2\text{CC}\equiv\text{CCO}_2\text{R}')]$ but the dinuclear platinum(II) compounds $[\text{Pt}_2(\text{CO})_2(\text{PR}_3)_2(\mu\text{-}\eta^1\text{-}\eta^1\text{-}\text{R}'\text{O}_2\text{CC}\equiv\text{CCO}_2\text{R}')]$ ($\text{R}' = \text{CH}_3, \text{PR}_3 = \text{PPh}_3$, **6**; $\text{R}' = ^t\text{Bu}, \text{PR}_3 = \text{PPh}_3$, **7**, PPh_2Bz **8**) or $[\text{Pt}_2(\text{CO})_2(\text{PR}_3)_2(\mu\text{-}\eta^1\text{-}\eta^1\text{-}^t\text{BuO}_2\text{CC}\equiv\text{CCO}_2^t\text{Bu})]$ ($\text{PR}_3 = \text{PCy}_3$, **9**, P^iPr_3 , **10**), the latter two having two “*cis*- $\text{Pt}(\text{CO})(\text{PR}_3)$ ” fragments bridged by bis- π alkyne interactions. The dinuclear platinum(II) complex **6** has been prepared by addition of dimethyl acetylenedicarboxylate to $\text{Pt}(\text{CO})_2(\text{PPh}_3)_2$,^{16a} as well as $[\text{Pt}_2(\text{CO})_2(\text{PCy}_3)_2(\mu\text{-}\eta^1\text{-}\eta^1\text{-}\text{CH}_3\text{O}_2\text{CC}\equiv\text{CCO}_2\text{CH}_3)]$ which is isostructural with **6**.^{16b}

The IR spectra of the three complexes **6–8** show two bands ($\nu(\text{C}=\text{O})$ B_1 and A_1) in the $2010\text{--}2050\text{ cm}^{-1}$ region, indicating CO groups terminally bonded to platinum(II); the spectra of **9** and **10** present a single absorption shifted to lower wavenumbers (1994 and 1999 cm^{-1} , respectively) in agreement with the increased basicity of the metal.^{14,17} All derivatives showed an additional strong absorption in the $1679\text{--}1703\text{ cm}^{-1}$ region due to $\nu(\text{C}=\text{O})$ of the carboxylate groups of the acetylene ligands. In this region no IR and Raman bands were found which could be assigned to the $\nu(\text{C}\equiv\text{C})$ of the coordinated alkyne.^{18,19}

The $^{195}\text{Pt}\text{-}\{^1\text{H}\}$, $^{31}\text{P}\text{-}\{^1\text{H}\}$ and $^{13}\text{C}\text{-}\{^1\text{H}\}$ NMR spectra of **8** are shown in Fig. 3a–c and selected data for **6–10** are collected in Table 2. Owing to the existence of isotope ^{195}Pt ($I = 1/2$, natural abundance 33.8%) each dinuclear complex contains two chem-

Table 2 Selected $^{195}\text{Pt}\text{-}\{^1\text{H}\}$, $^{31}\text{P}\text{-}\{^1\text{H}\}$ and ^{13}C NMR ^a data for complexes **6–10** at 25°C (δ/ppm , J/Hz)

	6	7	8	9	10
$\delta(\text{Pt})$	−5007	−5018	−4977	−4703	−4764
$^1J(\text{Pt}\text{-}\text{Pt})$	783.8	372.0	477.4		
$^2J(\text{Pt}\text{-}\text{Pt})$				505.4	537.1
$\delta(\text{P})$	19.40	18.87	9.25	29.64	43.57
$^1J(\text{P}\text{-}\text{Pt})$	2409	2873	2638	3169	3162
$^2J(\text{P}\text{-}\text{Pt})$	783.5	490.3	647.1		
$^3J(\text{P}\text{-}\text{Pt})$				−41.7	−17.5
$^3J(\text{P}\text{-}\text{P})$	163.9	116.1	149.6		
$^4J(\text{P}\text{-}\text{P})$				8.4	14.4
$\delta(\text{C})^a$	193.0	190.5	191.8	186.8	190.2
$^1J(\text{C}\text{-}\text{Pt})$	1235	1332	1258	1687	1678
$^2J(\text{C}\text{-}\text{Pt})$	8.0	<8	10.4		
$^3J(\text{C}\text{-}\text{Pt})$				−15.6	−14.3
$^2J(\text{C}\text{-}\text{P})$	3.5	<2	4.1	4.6	4.6
$^3J(\text{C}\text{-}\text{P})$	3.2	<2	3.3		
$^4J(\text{C}\text{-}\text{P})$				<0.5	<0.5
$^3J(\text{C}\text{-}\text{C})$	3.0	<2	4.0		
$^4J(\text{C}\text{-}\text{C})$				≈ 0.8	≈ 0.9

^a ^{13}C NMR data for the carbonyl ligands of the complexes enriched (>99%) in ^{13}C .

ically equivalent Pt atoms and is made of three isotopomers, *i.e.* 43.82% of the molecules are without ^{195}Pt , $2 \times 22.37\%$ contain one ^{195}Pt nucleus and 11.42% contain two ^{195}Pt nuclei. The observed spectrum is a superimposition of the spectra of each of these isotopomers taking into account their respective natural abundances. For example, the $^{31}\text{P}\text{-}\{^1\text{H}\}$ NMR spectrum of **8** (Fig. 3b) is composed of a singlet due to the A_2 spin system, 8 signals due to the AA' part of the $\text{AA}'\text{X}$ spin system, and 10 signals due to the AA' part of the $\text{AA}'\text{XX}'$ spin system, respectively. All spectra could be analysed using first order approximation and spectral simulation using the gNMR 4.0 program confirmed all values, except for the negative sign of the coupling constants $^3J(\text{P}\text{-}\text{Pt})$ and $^3J(\text{C}\text{-}\text{Pt})$ of **9** and **10**.

All spectra show a single resonance, with similar patterns of satellites, thus indicating that the dinuclear complexes have two chemically equivalent platinum environments with linear $\text{R}_3\text{P}\text{-}\text{Pt}\text{-}\text{Pt}\text{-}\text{PR}_3$ (**6–8**) or angular (**9**, **10**) arrangements. The coordination geometry about the metal centres of **6–8** could be viewed as a distorted square plane, in which the phosphines invariably prefer to be *trans* to the $\text{Pt}\text{-}\text{Pt}$ bond whilst the carbonyls are *cis*. There appears to be no obvious explanation for this preference apart from the steric problems raised if the phosphines were *cis* to the $\text{Pt}\text{-}\text{Pt}$ bond.

The rather low values for the $^1J(\text{Pt}\text{-}\text{Pt})$ coupling constant (372.0 and 477.4 Hz for **7** and **8**, respectively) compared with that for the isostructural dinuclear complex **6** (783.8 Hz) may be associated with the steric bulkiness of the di(*tert*-butyl)acetylenedicarboxylate ligand leading to an increase in the $\text{Pt}\text{-}\text{Pt}$ bond distance (see crystallographic section below). The relatively higher values of $^2J(\text{Pt}\text{-}\text{Pt})$ (505.4 and 537.1 Hz for **9** and **10**, respectively) may be due to additional metal–metal interactions. The values of the coupling constants $^3J(\text{P}\text{-}\text{Pt})$ and $^4J(\text{P}\text{-}\text{P})$ are respectively smaller than those of $^2J(\text{P}\text{-}\text{Pt})$ and $^3J(\text{P}\text{-}\text{P})$ found in **6–8**. On the basis of molecular orbital studies²⁰ it has been stated that the values of $^1J(\text{Pt}\text{-}\text{Pt})$, $J(\text{Pt}\text{-}\text{P})$

and $J(\text{P-P})$ should be larger for dinuclear complexes where the C-C bond is parallel to the Pt-Pt axis relative to complexes where the C-C bond is perpendicular to that axis. On comparing the data for complexes **6-10** (Table 2), this statement holds for ${}^2J(\text{Pt-Pt})$ vs. ${}^3J(\text{Pt-P})$ and ${}^3J(\text{P-P})$ vs. ${}^4J(\text{P-P})$, but not for ${}^1J(\text{Pt-Pt})$. Perhaps the best criterion for distinguishing between the two bonding modes of the alkyne ligand is the opposite sign of the $J(\text{Pt-P})$ and $J(\text{Pt-C})$ coupling constants: positive for **6-8** ($\mu\text{-}\eta^1\text{:}\eta^1\text{-type}$), negative for **9-10** ($\mu\text{-}\eta^2\text{:}\eta^2\text{-type}$).

Crystal structures of **8** and **9**

The molecular structures of **8** and **9** are shown in Fig. 4 and 5, respectively, and selected bond lengths and angles are collected in Table 3. Both complexes are dimers in which the two parts are related by a twofold axis. Alkyne coordination in **8** is of the $\mu\text{-}\eta^1\text{:}\eta^1\text{-type}$ with the C-C bond nearly collinear with the metal atoms. The structure is similar to that of $[\text{Pt}_2(\text{CO})_2(\text{PPh}_3)_3(\text{MeO}_2\text{CC}\equiv\text{CCO}_2\text{Me})]$.¹⁶ The Pt-Pt bond is longer in **8** (2.654 Å) than in the methyl derivative (2.635 Å). This is accompanied by a greater deviation from coplanarity of the atoms constituting the mean plane Pt-C(2)-C(2)#1-Pt#1 (mean deviation 0.134 Å for **8**, 0.03 Å for the methyl derivative). The latter is probably due to the bulkiness of the *tert*-butyl groups relative to the methyl groups which is reflected in the greater value of the dihedral angle C(3)-C(2)-C(2)#1-C(3)#1 (16.4° vs. 5.8°).

Alkyne coordination in **9** is of the $\mu\text{-}\eta^2\text{:}\eta^2\text{-type}$ with the C-C bond nearly perpendicular to the Pt-Pt axis (92°). The Pt-Pt distance is considerably longer (3.030 Å) than that in **8** and is relatively similar to that found in $[\text{Pt}_2(\text{PMe}_3)_4(\text{PhC}\equiv\text{CPh})]$ (2.905 Å)²¹ where the diphenyl acetylene ligand is coordinated perpendicularly to the Pt-Pt axis. The Pt-C(2)-C(2)#1-Pt#1 dihedral angle is also greater (101.9°) than that in **8** (26.1°) and in the Me derivative (6.6°). Its C(3)-C(2)-C(2)#1-C(3)#1 dihedral angle is similar to that of **8** (19.2 vs. 16.4°) and is therefore not indicative of a change in the hybridisation mode of the acetylenic carbon atoms.

An EHMO calculation²⁰ on the model complex $[\text{Pt}_2(\text{CO})_2(\text{PH}_3)_2(\text{HC}\equiv\text{CH})]$ with the perpendicular orientation of acetylene to the Pt-Pt axis (μ -bridging model) against the parallel one (di- σ model) has shown that the orientation of the acetylene ligand strongly affects the HOMO characteristics. The magnitude of the *s*-coefficient products for $s(\text{Pt})\text{-}s(\text{Pt})$ and

Table 3 Selected bond lengths [Å] and angles [°] for **8** and **9**^a

	8	9
Pt-C(1)	1.893(4)	1.859(4)
Pt-C(2)	2.044(3)	2.089(3)
C(2)-Pt#1		2.054(3)
Pt-P	2.3277(8)	2.3271(8)
Pt-Pt#1	2.6538(2)	3.0299(5)
O(1)-C(1)	1.126(5)	1.152(4)
O(2)-C(3)	1.213(4)	1.205(4)
O(3)-C(3)	1.341(4)	1.338(4)
O(3)-C(4)	1.469(5)	1.475(4)
C(2)-C(2)#1	1.334(6)	1.399(6)
C(2)-C(3)	1.485(4)	1.482(4)
C(4)-C(6)	1.488(7)	1.503(6)
C(4)-C(5)	1.511(6)	1.505(6)
C(4)-C(7)	1.516(7)	1.523(7)
P-C(10)	1.819(3)	1.838(3)
C(1)-Pt-C(2)	164.64(14)	111.62(14)
C(1)-Pt-C(2)#1		151.05(14)
C(1)-Pt-P	97.74(12)	99.29(11)
C(2)-Pt-P	96.99(8)	149.07(9)
C(1)-Pt-Pt#1	95.73(12)	121.36(11)
C(2)-Pt-Pt#1	70.03(8)	42.56(8)
P-Pt-Pt#1	165.65(2)	120.47(2)
C(2)#1-C(2)-C(3)	123.3(2)	136.2(2)
C(2)#1-C(2)-Pt	106.61(11)	68.9(2)
C(3)-C(2)-Pt	129.9(2)	125.2(2)
C(2)-C(3)-O(2)	126.8(3)	124.5(3)
C(2)-C(3)-O(3)	109.4(3)	110.6(3)
O(2)-C(3)-O(3)	123.7(3)	124.9(3)

^a Symmetry transformations used to generate equivalent atoms: for **8**: #1 = 1 - *x*, *y*, ½ - *z*; for **9**: #1 = 1 - *x*, ½ - *y*, *z*.

$s(\text{Pt})\text{-}s(\text{P})$ were found to be greater for the di- σ model (0.030 and -0.019, respectively) than those for the μ -bridging model (0.005 and -0.004, respectively). Therefore, the Pt-Pt σ bonding should be relatively weakened and the Pt-P σ bonding strengthened in the latter, which in turn should lower the ${}^1J(\text{Pt-Pt})$ and enhance the ${}^1J(\text{Pt-P})$ coupling constants. The Pt-Pt distance indeed increases with the increase in the Pt-C(2)-C(2)-Pt dihedral angle on going from the Me derivative to **8** and then to **9**. However, the corresponding values for ${}^1J(\text{Pt-Pt})$ do not follow the same sequence as shown in Table 2.

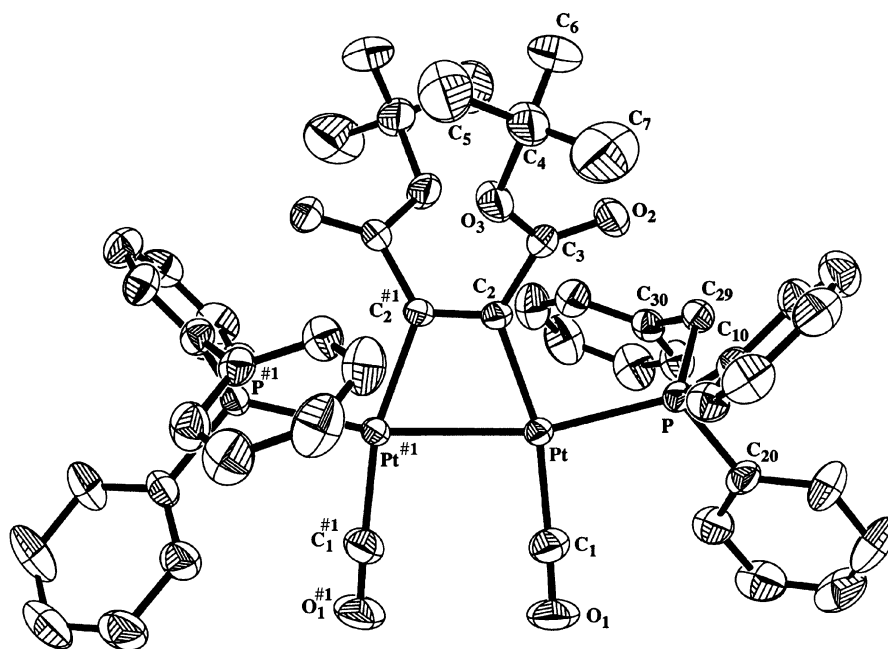


Fig. 4 Molecular structure of **8**. The symmetry transformation #1 stands for: 1 - *x*, *y*, ½ - *z*.

Experimental

General procedures

All manipulations were carried out under nitrogen atmosphere using standard Schlenk techniques. All solvents were dried by conventional methods and distilled prior to use. Infrared spectra of solids (KBr, Nujol mulls) and of CH_2Cl_2 solutions (KBr or CaF_2 cells) were recorded on Perkin-Elmer 983 or FT-IR-2000 spectrometers, and NMR spectra on Bruker AC 200 (^1H at 200.13 MHz, ^{31}P at 81.02 MHz and ^{13}C at 50.32 MHz), on Bruker WH 360 (^1H at 360.14 MHz, ^{13}C at 90.55 MHz) and on Bruker DRX 400 (^{31}P at 161.93 MHz, ^{13}C at 99.55 MHz and ^{195}Pt at 77.38 MHz) spectrometers. The chemical shifts (δ) are referenced to Me_4Si (^1H and ^{13}C), to external 85% H_3PO_4 (^{31}P) and to external Na_2PtCl_6 (^{195}Pt). The spectra of all nuclei (except ^1H) were ^1H decoupled. Simulations were made with the gNMR 4.0 program, taking into account only the relative population of platinum isotopomers since all samples for ^{13}C - $\{\text{H}\}$ NMR were enriched to $\geq 99\%$ ^{13}C .¹³

The compounds $[\text{Pt}_3(\mu\text{-CO})_3(\text{PR}_3)_3]$ ($\text{L} = \text{PPh}_3$,¹³ PPh_2Bz ,^{13,22} PCy_3 ,²³ and P^iPr_3 ,²³) were prepared by literature methods; the ^{13}C isotopically labeled derivatives were prepared similarly, using ^{13}C enriched to 99%. $\text{CH}_3\text{O}_2\text{CC}\equiv\text{CCO}_2\text{CH}_3$ and $^t\text{BuO}_2\text{CC}\equiv\text{CCO}_2^t\text{Bu}$ (Fluka) were used as purchased. Carbon monoxide ($>99\%$ ^{13}C) was used as received from I.C.M., Innerberg.

Spectroscopic evidence for the alkyne adduct $[\text{Pt}_3(\mu\text{-CO})_3(\text{PPh}_3)_3(\mu_3\text{-}^t\text{BuO}_2\text{CC}\equiv\text{CCO}_2^t\text{Bu})]$ (5)

A suspension of $[\text{Pt}_3(\mu\text{-CO})_3(\text{PPh}_3)_3]$ ($2 \div 3 \times 10^{-4}$ mol) in CD_2Cl_2 (0.4 ml) was cooled to -78°C and a slight excess of di(*tert*-butyl)acetylenedicarboxylate ($3 \div 4 \times 10^{-4}$ mol) in CD_2Cl_2 (0.3 ml) at -78°C was added *via* syringe. The resulting mixture was stirred for some minutes at low temperature ($<-50^\circ\text{C}$) and the red-brown solution examined by NMR spectroscopy was found to contain $[\text{Pt}_3(\mu\text{-CO})_3(\text{PPh}_3)_3(\mu_3\text{-}^t\text{BuO}_2\text{CC}\equiv\text{CCO}_2^t\text{Bu})]$. This adduct is stable for several days in cold solution, but all preparative-scale attempts to isolate it as a solid resulted in rearrangement to $[\text{Pt}_2(\text{CO})_2(\text{PPh}_3)_2(\mu\text{-}\eta^1\text{-}^t\text{BuO}_2\text{CC}\equiv\text{CCO}_2^t\text{Bu})]$ together with the starting material

$[\text{Pt}_3(\mu\text{-CO})_3(\text{PPh}_3)_3]$ according to NMR spectroscopic evidence of their solutions at higher temperature ($>-30^\circ\text{C}$). However, the dinuclear complex is the only species formed in the presence of excess acetylene.

Syntheses

$[\text{Pt}_2(\text{CO})_2(\text{PPh}_3)_2\{\mu\text{-}\eta^1\text{-}\eta^1\text{-CH}_3\text{O}_2\text{CC}\equiv\text{CCO}_2\text{CH}_3\}]$ (6). A suspension of $[\text{Pt}_3(\mu\text{-CO})_3(\text{PPh}_3)_3]$ (0.35 g, 0.24 mmol) in 20 ml of a 1 : 1 *n*-octane–benzene mixture was cooled to -10°C and dimethyl acetylenedicarboxylate (0.13 g, 0.91 mmol) was added *via* a syringe. The resulting mixture was stirred for 15 minutes in the cold and then for 2 h at room temperature. The obtained ochre-orange suspension was concentrated under vacuum to *ca.* 3 ml and heptane (10 ml) was added to complete precipitation. The solid was filtered, washed with cold heptane and recrystallised from dichloromethane–heptane at -20°C . Yield 0.276 g (69%) as ochre-yellow microcrystals of **1**. Mp $191\text{--}195^\circ\text{C}$ dec. (Found: C, 47.13; H, 3.20%. $\text{C}_{44}\text{H}_{36}\text{O}_6\text{P}_2\text{Pt}_2$ requires C, 47.49; H, 3.26%). IR (CH_2Cl_2): $\nu(\text{C}\equiv\text{O})$ 2052vs, 2015m; $\nu(\text{C}=\text{O})$ 1703s cm^{-1} .

$[\text{Pt}_2(\text{CO})_2(\text{PPh}_3)_2\{\mu\text{-}\eta^1\text{-}\eta^1\text{-}^t\text{BuO}_2\text{CC}\equiv\text{CCO}_2^t\text{Bu}\}]$ (7). A solution of di(*tert*-butyl)acetylenedicarboxylate (77 mg, 0.34 mmol) in dichloromethane (2 ml) was added to a stirred solution of $[\text{Pt}_3(\mu\text{-CO})_3(\text{PPh}_3)_3]$ (0.22 g, 0.15 mmol) in dichloromethane (15 ml) at -20°C . After 10 minutes in the cold the solution was stirred at room temperature for 30 minutes (the reaction progress was monitored by IR spectra). Evaporation of the solvent under reduced pressure gave a pale brown residue which was washed with cold pentane (2×3 ml) and crystallised from dichloromethane–heptane at -20°C . Yield 0.209 g (77%) as pale ochre microcrystals of **2**. Mp $167\text{--}168^\circ\text{C}$ dec. (Found: C, 49.93; H, 4.01%. $\text{C}_{50}\text{H}_{48}\text{O}_6\text{P}_2\text{Pt}_2$ requires C, 50.17; H, 4.04%). IR (CH_2Cl_2): $\nu(\text{C}\equiv\text{O})$ 2048vs, 2016m; $\nu(\text{C}=\text{O})$ 1692s cm^{-1} .

$[\text{Pt}_2(\text{CO})_2(\text{PPh}_2\text{Bz})_2\{\mu\text{-}\eta^1\text{-}\eta^1\text{-}^t\text{BuO}_2\text{CC}\equiv\text{CCO}_2^t\text{Bu}\}]$ (8). As for **7** starting with $[\text{Pt}_3(\mu\text{-CO})_3(\text{PPh}_2\text{Bz})_3]$ (0.37 g, 0.25 mmol) and di(*tert*-butyl)acetylenedicarboxylate (0.116 g, 0.51 mmol). Yield 0.328 g (72%) as pale yellow microcrystals. Mp $149\text{--}151^\circ\text{C}$ dec.

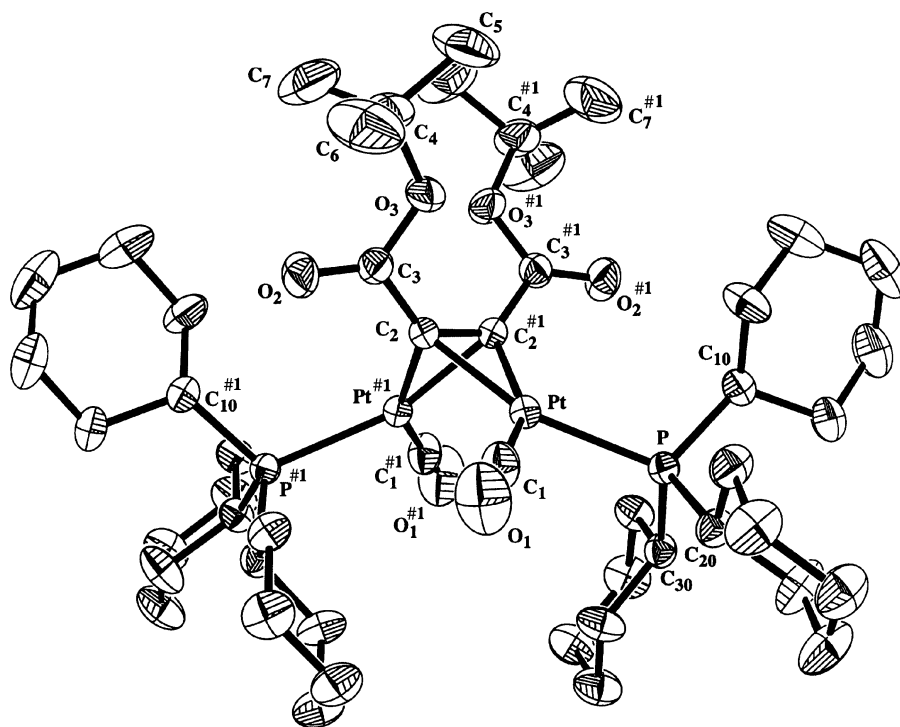


Fig. 5 Molecular structure of **9**. The symmetry transformation #1 stands for: $1 - x, \frac{1}{2} - y, z$.

Table 4 Crystallographic data for compounds **8** and **9**

	8	9
Molecular formula	C ₅₂ H ₅₂ O ₆ P ₂ Pt ₂	C ₅₀ H ₈₄ O ₆ P ₂ Pt ₂
<i>M</i>	1225.1	1233.30
Crystal system	Monoclinic	Tetragonal
<i>a</i> /Å	18.0590(7)	17.737(3)
<i>b</i> /Å	16.2947(7)	17.737(3)
<i>c</i> /Å	18.5105(8)	33.472(7)
β /°	116.2990(10)	
<i>U</i> /Å ³	4883.2(4)	10530(3)
<i>T</i> /K	293(2)	293(2)
Space group	<i>C</i> 2/ <i>c</i>	<i>I</i> 4 ₁ / <i>a</i>
<i>Z</i>	4	8
μ /mm ⁻¹	5.836	5.412
Reflections collected/unique	21362/8336	33314/4119
<i>R</i> _{int}	0.0311	0.0549
Final <i>R</i> ₁ , <i>wR</i> ₂ [<i>I</i> > 2 σ (<i>I</i>)]	0.0488, 0.0713	0.0192, 0.0355
(all data)	0.0544, 0.0719	0.0270, 0.0365

(Found: C, 50.83; H, 4.16%. C₅₂H₅₂O₆P₂Pt₂ requires C, 50.98; H, 4.28%). IR (CH₂Cl₂): ν (C=O) 2046vs, 2009m; ν (C=O) 1687s cm⁻¹.

[Pt₂(CO)₂(PCy₃)₂{ μ - η^2 : η^2 -^tBuO₂C \equiv CCO₂^tBu}] (**9**). As for **7** starting with [Pt₃(μ -CO)₃(PCy₃)₃] (0.26 g, 0.17 mmol) and di(*tert*-butyl)acetylenedicarboxylate (75 mg, 0.33 mmol). Yield 0.223 g (70%) as ivory coloured microcrystals. Mp 182–185 °C dec. (Found: C, 48.55; H, 6.91%. C₅₀H₈₄O₆P₂Pt₂ requires C, 48.69; H, 6.86%). IR (CH₂Cl₂): ν (C=O) 1994s; ν (C=O) 1679s cm⁻¹.

[Pt₂(CO)₂(PⁱPr₃)₂{ μ - η^2 : η^2 -^tBuO₂C \equiv CCO₂^tBu}] (**10**). A solution of di(*tert*-butyl)acetylenedicarboxylate (174 mg, 0.77 mmol) was added to a stirred solution of [Pt₃(μ -CO)₃(PⁱPr₃)₃] (0.46 g, 0.40 mmol) in cyclohexane (25 ml) at 5 °C. After 10 minutes at this temperature the solution was allowed to stir at room temperature. After 20 minutes a pale orange solution was obtained. Its IR spectrum showed the disappearance of the ν (CO) absorption at 1770 cm⁻¹ of the starting trinuclear cluster. Evaporation of the solvent under vacuum gave an oily residue which was treated with 4 ml of pentane and kept at -20 °C for 2 days. The pale yellow crystals were washed with cold pentane (3 \times 2 ml) and dried under vacuum. Yield 0.29 g (49%). Mp 116–118 °C dec. (Found: C, 38.90; H, 6.15%. C₃₂H₆₀O₆P₂Pt₂ requires C, 38.71; H, 6.09%). IR (CH₂Cl₂): ν (C=O) 1999vs; ν (C=O) 1681s cm⁻¹.

Crystal structures

Crystal data for 8. A yellow crystal the habitus of which consisted of a {110} prism, a { $\bar{1}12$ } pinacoid and a { $\bar{1}\bar{1}2$ } bevel face was brought onto a Bruker SMART CCD system equipped with Mo radiation. A hemisphere of reflections were collected as ω scans over twelve hours. Using the SAINT package,²⁴ lattice constants were optimized (Table 4) and intensities were integrated and corrected for Lorentz and polarization effects. A semi-empirical absorption correction based on ψ -scans was computed with the help of the XPREP program.²⁵ The structure was solved with the help of DIRDIF 96,²⁶ and refined by means of SHELXTL 5.05.²⁵ All non-hydrogen atoms were refined anisotropically, and all hydrogens were made to ride on their associated carbons.

Crystal data for 9. A yellow crystal the habitus of which consisted of a not fully developed {112} dipyrmaid was measured on a Stoe IPDS system equipped with Mo radiation. A crystal-image plate distance of 80 mm was chosen and 200 images, in oscillation steps of 1°, were exposed for five minutes

each. The intensities were corrected for Lorentz and polarization effects and an absorption correction based on the crystal habitus was carried out as well. The structure was solved with the help of DIRDIF 96,²⁶ and refined by means of SHELXTL 5.05.²⁵ All non-hydrogen atoms were refined anisotropically, and all hydrogens were made to ride on their associated carbons.

CCDC reference numbers 163707 and 163708.

See <http://www.rsc.org/suppdata/dt/b1/b103306a/> for crystallographic data in CIF or other electronic format.

Acknowledgements

We thank the Swiss National Science Foundation and Murst Cofin-2000 for financial support.

References

- H. C. Clark and V. K. Jain, *Coord. Chem. Rev.*, 1984, **55**, 151.
- R. Whyman, *Transition Metal Clusters*, B. F. G. Johnson, ed., Wiley, New York, 1980, pp. 471–608.
- E. L. Muetterties, T. N. Rodin, E. Band, C. F. Bruker and W. R. Pretzer, *Chem. Rev.*, 1979, **79**, 91.
- P. Braunstein and J. Rose, in *Stereochemistry of Organometallic and Inorganic Compounds*, I. Bernal, ed., Elsevier, Amsterdam, 1988, vol. 3.
- K. H. Dahmer, A. Moor, R. Naegli and L. M. Venanzi, *Inorg. Chem.*, 1991, **30**, 4285.
- A. Albinati, A. Moor, P. S. Pregosin and M. L. Venanzi, *J. Am. Chem. Soc.*, 1982, **104**, 7672.
- A. Albinati, K.-H. Dahmer, A. Togni and M. L. Venanzi, *Angew. Chem.*, 1985, **97**, 760.
- D. M. P. Mingos and T. Slee, *J. Organomet. Chem.*, 1990, **394**, 679.
- A. D. Burrows and D. M. P. Mingos, *Coord. Chem. Rev.*, 1996, **154**, 19.
- M. J. S. Dewar, *Bull. Soc. Chim. Fr.*, 1951, **18**, C79; J. Chatt and L. A. Duncanson, *J. Chem. Soc.*, 1953, 2339; M. J. S. Dewar, R. C. Haddon, A. Komorniki and H. Rzepa, *J. Am. Chem. Soc.*, 1977, **99**, 377; M. J. S. Dewar and G. P. Ford, *J. Am. Chem. Soc.*, 1979, **101**, 783.
- D. M. Hoffman, R. Hoffman and C. R. Fisel, *J. Am. Chem. Soc.*, 1982, **104**, 3858 and references therein.
- R. S. Dickson and G. N. Pain, *J. Chem. Soc., Chem. Commun.*, 1979, 277; N. M. Boag, M. Green and F. G. A. Stone, *J. Chem. Soc., Chem. Commun.*, 1980, 1281.
- R. Ros, A. Tassan, G. Laurency and R. Roulet, *Inorg. Chim. Acta*, 2000, **303**, 94.
- R. Ros, G. Facchin, A. Tassan, R. Roulet, G. Laurency and F. Lukas, *J. Cluster Sci.*, 2001, **12**, 99.
- gNMR, version 4.0, Cherwell Scientific Publishing Limited, Oxford, 1995–1997.
- (a) Y. Koie, S. Shinoda, Y. Saito, B. J. Fitzgerald and C. G. Pierpont, *Inorg. Chem.*, 1980, **19**, 770; (b) G. J. Spivak and R. J. Puddephatt, *J. Organomet. Chem.*, 1998, **551**, 383.
- S. Braterman, *Metal Carbonyl Spectra*, Academic Press, New York, 1975.
- H. C. Clark and L. E. Manzer, *Inorg. Chem.*, 1974, **13**, 1291.
- N. M. Boag, M. Green, D. M. Grove, J. A. K. Howard, J. L. Spencer and F. G. A. Stone, *J. Chem. Soc., Dalton Trans.*, 1980, 2170 and references therein.
- Y. Koie, S. Shinoda and Y. Saito, *Inorg. Chem.*, 1981, **20**, 4408.
- N. M. Boag, J. Browning, C. Crocker, P. L. Goggin, R. J. Goodfellow, M. Murray and J. L. Spencer, *J. Chem. Res. (M)*, 1978, 2962.
- J. Chatt and P. Chini, *J. Chem. Soc. A*, 1970, 1538.
- K. H. Dalmer, A. Moor, R. Naegli and L. M. Venanzi, *Inorg. Chem.*, 1991, **30**, 4285.
- SAINT, Program for the Reduction of Data from an Area Detector, version 4.05, Bruker Analytical X-Ray Instruments, Inc., Madison, WI, 1996.
- G. M. Sheldrick, SHELXTL 5.05, Bruker Analytical X-Ray Instruments, Inc., Madison, WI, 1996.
- P. T. Beurskens, G. Beurskens, W. P. Bosman, R. de Gelder, S. García-Granda, R. O. Gould, R. Israël and M. M. Smits, The DIRDIF 96 System of Programs, Laboratorium voor Kristallografie, Katholieke Universiteit Nijmegen, 1996.